

Application of optogenetic Amyloid- β distinguishes between metabolic and physical damages in neurodegeneration

Chu Hsien Lim^{1†}, Prameet Kaur^{1†}, Emelyne Teo¹, Vanessa Yuk Man Lam¹, Fangchen Zhu¹, Caroline Kibat^{1,2,3}, Jan Gruber^{1,4}, Ajay S Mathuru^{1,2,3}, Nicholas S Tolwinski^{1*}

¹Science Division, Yale- NUS College, Singapore, Singapore; ²Institute of Molecular and Cell Biology (IMCB), Singapore, Singapore; ³Department of Physiology, YLL School of Medicine, Singapore, Singapore; ⁴Department of Biochemistry, National University of Singapore, Singapore, Singapore

Abstract The brains of Alzheimer’s disease patients show a decrease in brain mass and a preponderance of extracellular Amyloid- β plaques. These plaques are formed by aggregation of polypeptides that are derived from the Amyloid Precursor Protein (APP). Amyloid- β plaques are thought to play either a direct or an indirect role in disease progression, however the exact role of aggregation and plaque formation in the aetiology of Alzheimer’s disease (AD) is subject to debate as the biological effects of soluble and aggregated Amyloid- β peptides are difficult to separate in vivo. To investigate the consequences of formation of Amyloid- β oligomers in living tissues, we developed a fluorescently tagged, optogenetic Amyloid- β peptide that oligomerizes rapidly in the presence of blue light. We applied this system to the crucial question of how intracellular Amyloid- β oligomers underlie the pathologies of A. We use *Drosophila*, *C. elegans* and *D. rerio* to show that, although both expression and induced oligomerization of Amyloid- β were detrimental to lifespan and healthspan, we were able to separate the metabolic and physical damage caused by light-induced Amyloid- β oligomerization from Amyloid- β expression alone. The physical damage caused by Amyloid- β oligomers also recapitulated the catastrophic tissue loss that is a hallmark of late AD. We show that the lifespan deficit induced by Amyloid- β oligomers was reduced with Li⁺ treatment. Our results present the first model to separate different aspects of disease progression.

***For correspondence:**
nicholas.tolwinski@yale-nus.edu.sg

[†]These authors contributed equally to this work

Competing interests: The authors declare that no competing interests exist.

Funding: See page 17

Received: 09 October 2019

Accepted: 18 March 2020

Published: 31 March 2020

Reviewing editor: Matt Kaeberlein, University of Washington, United States

© Copyright Lim et al. This article is distributed under the terms of the [Creative Commons Attribution License](https://creativecommons.org/licenses/by/4.0/), which permits unrestricted use and redistribution provided that the original author and source are credited.

Introduction

Alzheimer’s disease (AD) is a debilitating, age-associated, neurodegenerative disease which affects more than 46.8 million people worldwide and represents the 6th leading cause of death in the United States of America (Ahn et al., 2001; De-Paula et al., 2012; Hawkes, 2016; Kumar et al., 2015; Zhang et al., 2011). Despite extensive efforts over the last 50 years, no disease-modifying therapy has been found and, most recently, several high-profile Phase III clinical trials have failed (Anderson et al., 2017; Lim and Mathuru, 2018; Park et al., 2018). The AD clinical trial landscape has largely been dominated by the amyloid cascade hypothesis, with more than 50% of the drugs targeting amyloid beta (A β) in Phase III trials alone (Cummings et al., 2018). The amyloid cascade hypothesis, in its original form, posits the deposition of A β , in particular the extracellular A β plaque, as the main driver of AD (Hardy and Higgins, 1992). However, the causative role of A β plaques has recently been challenged, because of the failure of numerous interventions targeting A β plaques in Phase III trials and the observation of A β plaques in brains of non-AD symptomatic individuals (Cummings, 2018). Model organisms ranging from nematodes to mice have further shown that AD pathology can be modeled in the absence of obvious A β plaques (Duff et al., 1996; Fong et al.,

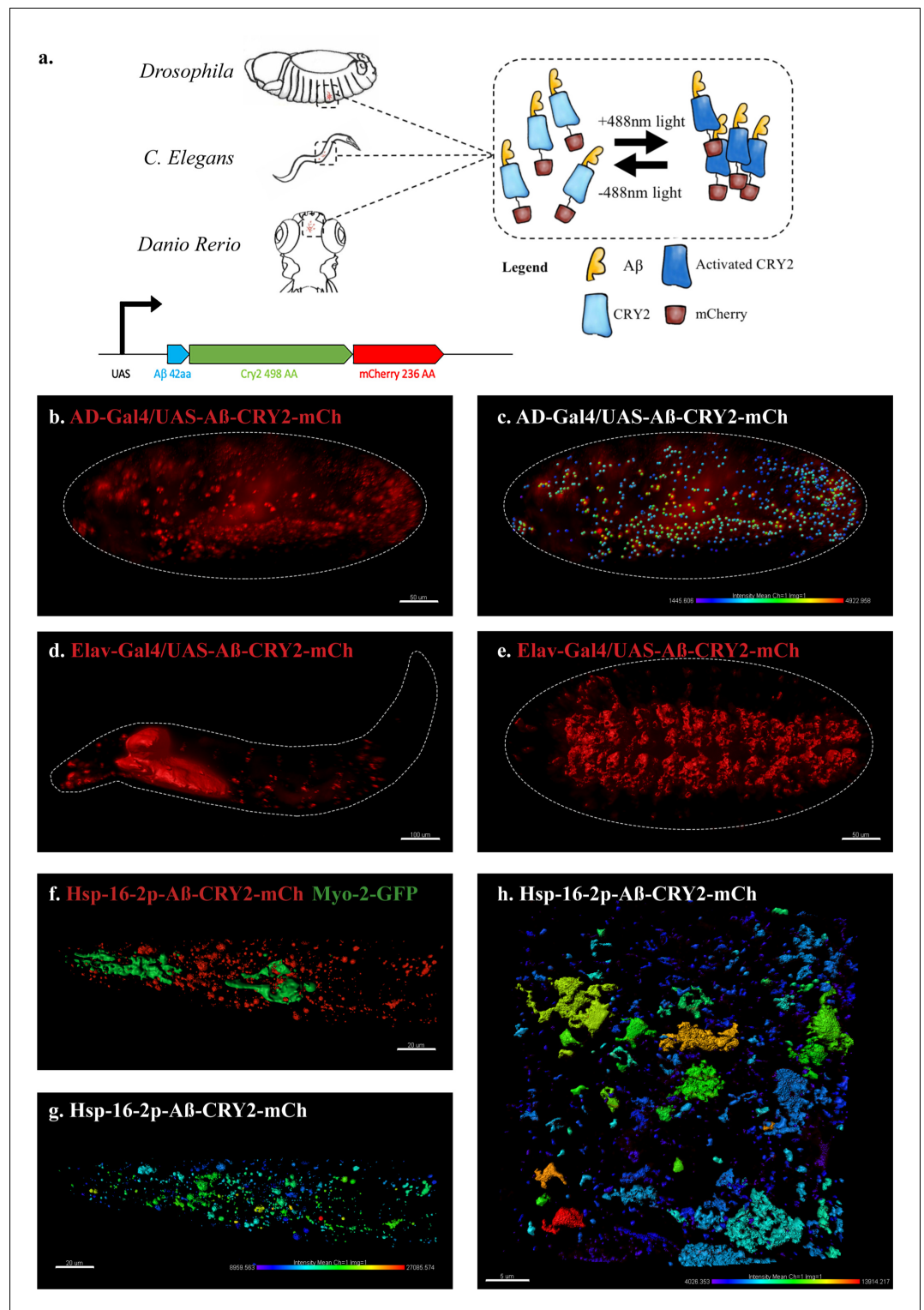


Figure 1. An in vivo, light-dependent, oligomerization switch for the formation or dissolution of Aβ aggregates in the fruit fly and nematode. (a) A schematic of the strategy and a relative size comparison of the three components of UAS-Aβ-CRY2-mCh. (b) Expression of AD-Gal4/UAS-Aβ-CRY2-mCh in a *Drosophila* embryo. (c) Mean intensity of aggregates in the same AD-Gal4/UAS-Aβ-CRY2-mCh *Drosophila* embryo. (d and e) Expression of Elav-Gal4/UAS-Aβ-CRY2-mCh in a *Drosophila* larva and embryo. (f) Expression of hsp-16-2 p-Aβ-CRY2-mCh in heat-shocked *C. elegans* with *myo-2-gfp* marker, that marks its pharyngeal pump and serves as an indicator for positive Figure 1 continued on next page

Figure 1 continued

microinjection. (g and h) Mean intensity of aggregates in the hsp-16-2 p-A β -CRY2-mCh in *C.elegans* under 20x and 63x magnification of the confocal microscope; 63x image was processed using the Zeiss Airyscan.

The online version of this article includes the following figure supplement(s) for figure 1:

Figure supplement 1. Transgenic *Drosophila* model expressing A β -CRY2-mCh.

Figure supplement 2. Exposure to light drives A β aggregation in *C. elegans* strains 24 hr post heat-shock.

Figure supplement 3. Light-induced A β aggregation in *Drosophila* embryos resulted in distinct developmental defects.

Figure supplement 4. Thioflavin T (ThT) staining showing the A β aggregation transgenic *Drosophila* embryos ubiquitously expressing A β -CRY2-mCh.

2016; Teo et al., 2019). These observations point to a different mechanism for A β neurotoxicity perhaps through A β 's intracellular accumulation (LaFerla et al., 2007).

Amyloid plaques are macroscopic extracellular protein aggregates, but intracellular A β must function in smaller units of peptides, oligomers or aggregates. Of these, soluble A β oligomers appear to be the main toxic species in AD (Ferreira and Klein, 2011). For example, A β oligomers have been shown to induce neurotoxic effects including memory loss in transgenic animal models reviewed in Mroczko et al. (2018). These studies, however, mostly rely on in vitro injection of synthetic A β oligomers or oligomers extracted from AD brains (Mroczko et al., 2018). There is currently a lack of tools that can directly control A β oligomerization in vivo, which would allow direct examination of the effects of A β oligomerization.

Here, we describe an optogenetic method to study Amyloid- β (A β) protein oligomerization in vivo in different model organisms and apply it to delineating mechanisms of disease progression. Optogenetics hinges on light responsive proteins that can be fused to genes of interest, allowing for the spatial and temporal regulation of proteins in a highly precise manner. Temporal-spatial control is achieved simply by the exposure of the target system to lights of a specific wavelength, without the need to introduce other external agents (Fenno et al., 2011; Möglich and Moffat, 2010). One such optogenetic protein, a modified version of the *Arabidopsis thaliana* cryptochrome 2 (CRY2) protein, oligomerizes into photobodies quickly and reversibly in the presence of blue light at 488 nm (Más et al., 2000). In cultured cells, expression of the photolyase homology region of CRY2 fused to mCherry led to puncta within 10 s of exposure to blue light and these puncta dispersed within minutes (Bugaj et al., 2013). This basic unit of CRY2-mCherry attached to a variety of proteins have, for instance, been used to study cortical actin dynamics in cell contractility during tissue morphogenesis, the dynamics of Wnt and EGF signaling, plasma membrane composition and transcriptional regulation (Bugaj et al., 2018; Bugaj et al., 2015; Guglielmi et al., 2015; Huang et al., 2017; Idevall-Hagren et al., 2012; Johnson et al., 2017; Kaur et al., 2017; Kennedy et al., 2010).

Results

To address the role of aggregation of intracellular A β in the pathophysiological effects of AD, we developed a light-inducible system for use in model organisms. Specifically, we generated an in vivo, light-dependent, oligomerization switch for the formation and dissolution of A β oligomers in *Drosophila melanogaster*, *Caenorhabditis elegans* and *Danio rerio* (Figure 1a). This optogenetically-driven model allowed the visualization of microscopic A β oligomerization and addressed the question of their relationship to A β pathogenesis with spatiotemporal precision.

Generation of transgenic models with light-inducible intracellular A β oligomerization in model organisms

We generated transgenic animals expressing the 42-amino-acid human A β peptide (A β 1–42) fused to Cryptochrome 2 and the fluorescent protein mCherry (A β -CRY2-mCh, Figure 1a, please note the relative sizes). *Drosophila* lines were under the control of the GAL4/UAS system (Brand and Perrimon, 1993) and expressed either ubiquitously via AD-Gal4 driver (Figure 1b–c) or specifically in neurons using Elav-Gal4 driver (Figure 1d–e, Figure 1—figure supplement 1). *C. elegans* lines were made with the heat shock promoter (Figure 1f–h, Figure 1—figure supplement 2). In order to observe oligomerization and clustering of intracellular A β , we took a live imaging approach in

Drosophila embryos using a lightsheet microscope with a 488 nm laser activating CRY2 and the 561 nm laser imaging mCh over time. We observed clusters of mCh fluorescence forming in embryos exposed to 488 nm light, but fewer in embryos that were not exposed to blue light (**Figure 1—figure supplement 3, Videos 1–2**). The intensity of the clusters was quantified using Imaris quantification software to show the intensity of oligomer formation (**Figure 1c**, note color scale for cluster intensity).

We proceeded to test the effectiveness of light induced clustering of A β -CRY2-mCh in *C. elegans*. As this construct is driven by a heat shock promoter, worms were heat shocked at 35°C for 90 min followed by resting at 20°C before being immobilized and imaged using confocal microscopy (**Figure 1f–h**). We observed an increase in clusters in worms exposed to blue light over their siblings not exposed to blue light. The results were quantified as fluorescence intensity and represented in (**Figure 1h**) showing the formation of A β clusters.

Induction of chaperones from heat-shock can impact the dynamics of A β . In particular, heat-shock treatment in another transgenic *C. elegans* strain, CL4176, reduced A β -mediated paralysis and A β oligomerization (**Winblad, 1989; Wu et al., 2010**). Overexpression of chaperone protein suppressed A β -toxicity in *C. elegans* (**Fonte et al., 2008**). The use of hsp-16 promoter in the transgenic *C. elegans*, which requires heat-shock induction, may hence be a limitation of our current approach. In view of this limitation, we performed several other controls to understand the impact of heat-shock treatment on A β dynamics, and whether or not heat-shock treatment itself contributes to the metabolic and phenotypic detriments observed in the transgenic animals.

To understand how heat-shock treatment may impact the dynamics of A β in our transgenic strains, we compared the dynamics of A β between the transgenic A β worms with and without heat shock. We found that transgenic animals in both heat-shock (A β HS L) and non-heat-shock (A β -HS L) condition expressed detectable A β -CRY2-mCh protein (**Figure 1—figure supplement 2**), however animals that had been heat-shocked had significantly higher A β levels compared to non-heat-shocked animals, suggesting that heat-shock, as intended, drove higher level of A β expression and that this was not compensated for by secondary induction of chaperones.

Even though the CRY2 system predominantly oligomerizes, we also observed the formation of intracellular A β aggregates, using a direct stain for A β aggregates (**Figure 1—figure supplement 4**). Importantly, we observed that A β aggregation was not reversible as had previously been observed for signaling molecules (**Huang et al., 2017; Johnson et al., 2017; Kaur et al., 2017**), rather CRY2 appeared to initiate clustering leading to A β bundles that did not come apart once blue light was turned off. We further confirmed that turning on blue light alone without the transgene expression did not lead to any A β expression or cluster formation (**Figure 1—figure supplement 2b, Ab HS L vs Ab -HS L**), suggesting that the oligomerization process was CRY2-specific and not an artifact of



Video 1. Elav-Gal4/UAS-A β -CRY2-mCh embryos kept in the dark and imaged for neurons in red mCherry and glial cells Repo-QF2 >QUAS GFP. Blue laser power kept low to allow imaging of glial cells, but not high enough to activate aggregation.

<https://elifesciences.org/articles/52589#video1>



Video 2. Elav-Gal4/UAS-A β -CRY2-mCh embryos exposed to light and imaged for neurons in red mCherry and glial cells Repo-QF2 >QUAS GFP. Blue laser power at higher setting to allow imaging of glial cells and activate aggregation.

<https://elifesciences.org/articles/52589#video2>

light. We performed FRAP experiments to establish the stability of the A β clusters (**Figure 2**). When compared to an unrelated CRY2 construct, we observed a very slow recovery for A β -CRY2-mCh compared to Arm-CRY2-mCh (**Figure 2**; *Kaur et al., 2017*). Together, our results showed that the A β -CRY2-mCh transgene was functional in both organisms, with a high specificity to blue light inducing irreversible oligomerization of A β .

Light-inducible A β oligomerization causes lifespan and behavioral deficits in transgenic models

To test the functionality of A β -CRY2-mCh, we next looked for phenotypes associated with light-induced intracellular A β oligomerization. We performed lifespan studies to assess the effects of A β -CRY2-mCh by expressing A β -CRY2-mCh either ubiquitously (AD-Gal4) or specifically in the nervous system (Elav-Gal4). Newly eclosed adult flies were separated into two groups in each case, one of which was exposed to ambient white light and the other kept in the dark. In both cases, flies exposed to light died much more quickly with half the mean and maximum lifespans (**Figure 3a–b**) compared to those reared in the dark. We extended this analysis to *C. elegans*, though starting at Day 6 due to the heat-shock manipulation step. Under light conditions, *C. elegans* showed markedly decreased lifespans as compared to the transgenic *C. elegans* kept in dark conditions (**Figure 3c**). Most significantly, we observed that the lifespan decrease was reversible, as taking animals exposed to light for 24 days and moving them into darkness showed a recovery of their lifespan, or a rescue (**Figure 3a–b**). To ensure that these reduced lifespans were physiological, we examined the fitness of the animals. Fitness was severely decreased in light-exposed flies and worms as quantified by fertility and locomotive assays (**Figure 3—figure supplement 1**). Interestingly, light-induced A β oligomerization caused further impairment in sensorimotor function of transgenic A β nematodes (**Figure 3—figure supplement 1c**). These results suggested that light-induced oligomerization of A β not only affected lifespan and fitness, but also impaired complex sensorimotor function and behavior.

Light-inducible A β oligomerization leads to physical and metabolic damage in transgenic models

The lethality mediated by light-induced A β oligomerization led us to examine the morphological effects of A β -CRY2-mCh clustering during embryonic stages in *Drosophila*. Embryos expressing A β in only the nervous system developed at a normal pace and did not show any morphogenetic defects and even hatched in the absence of blue light (**Video 1**). In contrast, sibling embryos exposed to blue laser light arrested in late neurogenesis stages where the central nervous system stopped developing and the embryos died (**Video 2** and **Figure 4, Figure 1—figure supplement 3** and **Figure 4—figure supplement 1**). These embryos showed a variety of abnormalities in the positioning of neurons and glial cells (Compare to complete normal development, **Video 3**) suggesting that light-induced A β oligomerization caused physical, structural damage that affects neuronal development.

The severity of the physical damage phenotype in embryos exposed to blue light (**Figure 4a–d'**) led us to investigate the differences in mechanism between the two conditions by exploring inflammatory response, mitochondrial health and oxidative damage. Expression of A β alone, without light-induced A β oligomerization, led to a small increase in inflammatory markers (**Figure 4e**; *Westfall et al., 2018*). In embryos exposed to light, two of these markers increased to a much greater level (**Figure 4e**). We observed a significant reduction in the number of mitochondria in light-treated A β animals (**Figure 4f**). Markers of oxidative damage in light and dark exposed *C. elegans* showed differential expression of antioxidant defense genes, specifically Catalase, Trx-2 and Sod-3, suggestive of the occurrence of oxidative stress induced by A β oligomerization (**Figure 5**). These results suggested that light-induced A β oligomerization phenocopied many of the hallmarks of AD.

We proceeded to look at light-induced A β oligomerization in metabolic impairments in transgenic *C. elegans*. Heat-shocked mutants exposed to light (A β HS L) had lower ATP levels compared to the non-transgenic control (Ctrl -HS D) (**Figure 6**). However, heat-shocked mutants in the dark condition (A β HS D) did not show any significant differences in ATP level compared to the non-transgenic control. This result suggested that presence of A β alone is insufficient to induce ATP deficits, and that

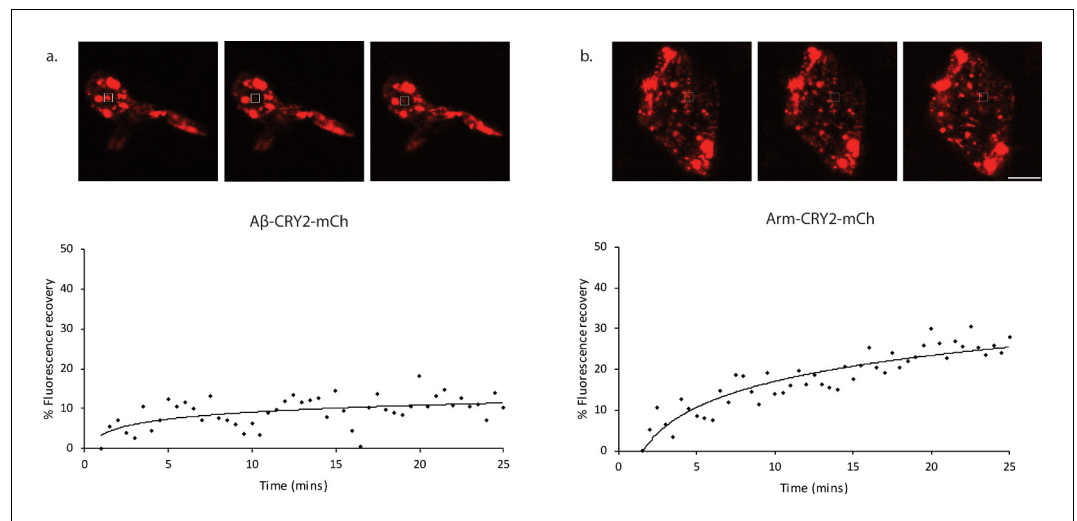


Figure 2. Fluorescence recovery after photobleaching (FRAP) analysis of A β -CRY2-mCh expressing cells compared to Arm-CRY2-mCh expressing cells in *Drosophila* gut. Images and percentage fluorescence recovery after bleaching of (a) A β -CRY2-mCh expressing intestinal stem cells from *esg-Gal4, UAS-GFP; UAS-A β -Cry2-mCh* flies and (b) Arm-CRY2-mCh expressing stem cells from *esg-Gal4, UAS-GFP; UAS-Arm-Cry2-mCh* flies. A β -Cry2-mCh showed a much slower recovery of fluorescence post-bleaching as compared to an unrelated CRY2 construct (Arm-CRY2-mCh). Scale bar represents 5 μ m.

light-induced oligomerization of A β is required for the defect to manifest. A β expression alone was also insufficient to affect the nematodes' maximum respiratory capacity, as heat-shocked mutants in the dark condition (A β HS D) did not display differences in maximum and spare respiration capacity compared to control animals (Ctrl -HS D). However, light-induced A β oligomerization significantly reduced maximum respiration capacity in *C. elegans*. Heat-shocked mutants in the light condition (A β HS L) displayed significantly lower maximum and spare respiration capacity compared to controls (Ctrl -HS D) and to heat-shocked mutants in the dark condition (A β HS D) (Figure 6b–d). Together, these results highlighted the metabolic differences between the two conditions and showed that metabolic deficits were mediated by light-induced A β oligomerization.

To further examine whether the metabolic deficits in transgenic *C. elegans* were mediated by heat-shock treatment, we included a heat-shocked non-transgenic control in the metabolic and phenotypic assays. We found that heat-shock treatment does not affect ATP levels in the control animals, suggesting that the ATP detriment was a result of A β expression, but not heat-shock treatment (Figure 6a). On the other hand, heat-shock treatment appears to reduce the respiratory capacity of the control animals, suggesting that the decline in respiratory capacity was mediated by both heat-shock and A β expression (Figure 6c). Comparing the heat-shocked transgenic animals in light and dark conditions, we found that light treatment, which induces oligomerization, worsened the phenotypic and metabolic detriments in the transgenic animals. This suggested that regardless of the effects of heat-shock and chaperone induction, oligomerization still negatively impacted the phenotypes.

Light-inducible A β lifespan decrease is rescued by Li⁺

The drug Li⁺ is used for treatment of neurological conditions (Licht, 2012). A high drinking water Li⁺ concentration correlated with lower human mortality (Zarse et al., 2011), and Li⁺ increased the lifespan of *C. elegans* and *Drosophila* (Castillo-Quan et al., 2016; McColl et al., 2008; Tam et al., 2014; Teo et al., 2020a; Teo et al., 2020b; Zarse et al., 2011). The molecular mechanisms by which Li⁺ functions include inhibition of inositol monophosphatase (IMPA) and glycogen synthase kinase-3 (GSK-3) (Kerr et al., 2018), reduction of oxidative damage (Kasuya et al., 2009; Kerr et al., 2017; Khan et al., 2015) and longevity via a GSK-3/NRF-2 dependent, hormetic mechanism (Castillo-Quan et al., 2016). Among the mechanisms for neuroprotection, the Wnt signaling pathway plays a role in modulating AD pathology and its progression (De Ferrari et al., 2003; Jin et al., 2017;

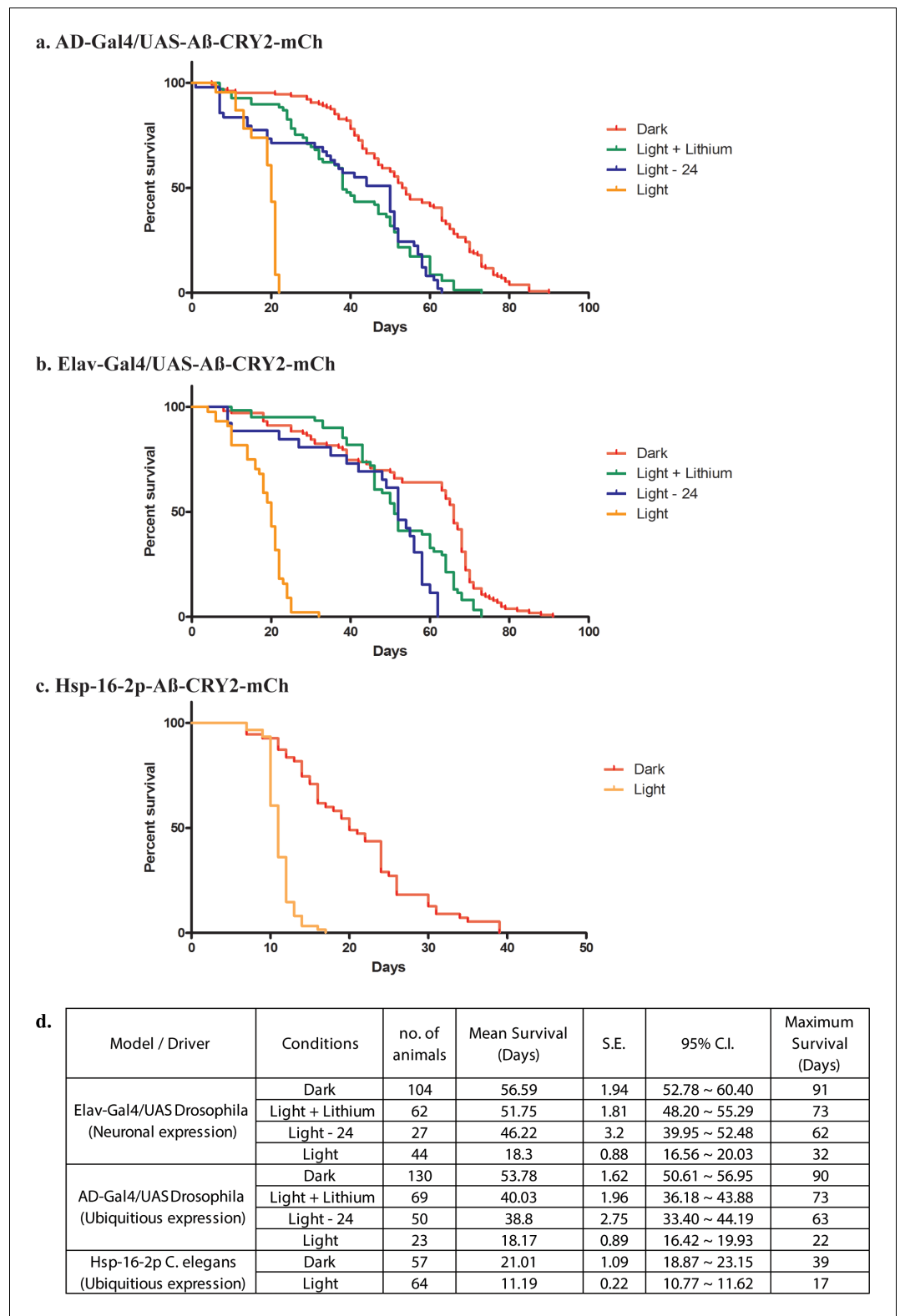


Figure 3. Analysis of lifespans in transgenic A β -aggregation *C. elegans* and *Drosophila* and adult models. (a) Kaplan-Meier survival curves of transgenic A β *Drosophila* adults driven by AD-Gal4 kept in the dark, exposed to light, exposed to light for 24 days then moved to the dark and exposed to light but fed with a lithium-supplemented diet. (b) Kaplan-Meier survival curves of transgenic A β *Drosophila* adults driven by Elav-Gal4 kept in the dark, exposed to light, exposed to light for 24 days then moved to the dark and exposed to light but fed with
Figure 3 continued on next page

Figure 3 continued

a lithium-supplemented diet. (c) Kaplan-Meier survival curves of control non-heat shocked nematodes, transgenic A β heat-shocked worms with the hsp-16-2 p promoter kept in the dark and transgenic A β heat-shocked worms with the hsp-16-2 p promoter kept in the light; those in light show a significantly shortened lifespan (overall significance by log-rank test: **** $p < 0.0001$) (d) Table showing number of samples used with the mean and maximum survival times for all conditions.

The online version of this article includes the following figure supplement(s) for figure 3:

Figure supplement 1. A β -CRY2-mCh expressing transgenic *C. elegans* and *Drosophila* reared in light showed signs of reduced fitness.

Parr et al., 2015; Toledo and Inestrosa, 2009). Activation of Wnt signaling through lithium (Li⁺) treatment attenuated A β aggregation and increased the lifespan of A β models (*Toledo and Inestrosa, 2009*). By inhibiting the enzyme glycogen synthase kinase-3 (GSK-3), Li⁺ compounds drive the downstream production of intracellular β -catenin activating the Wnt- β -catenin signaling pathway (*Klein and Melton, 1996*). Li⁺ treatment through Wnt activation also rescued behavioral impairment and neurodegeneration induced by A β fibrils (*De Ferrari et al., 2003*). Taken together, these studies point to a putative AD therapeutic intervention through Li⁺. To test the usefulness of optogenetic A β for drug testing, we supplemented the food for *Drosophila* expressing A β -CRY2-mCh with Li⁺. *Drosophila* exposed to light, but consuming Li⁺ had significantly increased lifespans, suggesting both a rescue effect induced by Li⁺ (*Figure 3a–b*), and that the optogenetic model can be used for inducible expression drug testing. Rapid drug testing can be also be achieved through cell culture. We extended this assay to HEK293 cells transfected with A β -CRY2-mCh where A β clusters formed upon stimulation with blue light (*Figure 7a*). The number of clusters per cell was greatly reduced by the addition of Li⁺ or the specific GSK3 inhibitor CHIR99021, but CHIR99021 additionally reduced the signal intensity of the clusters (*Figure 7b–c*, quantified 7d). These data demonstrated the potential use of the optogenetics system for drug testing.

Finally, we also extended these findings to a vertebrate system. We generated a zebrafish permanent line with UAS:A β -CRY2-mCh in the transgenic *TgBAC(gng8:GAL4)^{c416}* background (*Hong et al., 2013*) that limited expression to a few cells. We observed a diffuse mCh fluorescence in a small subset of neurons in the olfactory epithelium, the interpeduncular nucleus and in a few neurons sparsely distributed in the forebrain at 5 dpf. Upon blue light exposure (488 nm) the detectable intensity of the fluorescence increased rapidly (*Figure 8—figure supplement 1*). Several neurons among those expressing appeared to bleb and began to die within 40 to 50 min of initial exposure to the blue light (*Video 4*). Such damage was not observable in matched controls expressing A β -mCh driven by a CMV promoter lacking the CRY2 protein (*Video 5*). Our approach leads to the expression of A β -CRY2-mCh in only a small subset of neurons making analysis of AD hallmarks difficult, so we used transient expression of A β -CRY2-mCh driven by a ubiquitin promoter in 48 hr old embryos to quantify the effects of light-induced A β oligomerization on mitochondria health and metabolic deficits. Similar to the impairments observed in *C. elegans*, A β -CRY2-mCh expressing embryos showed lower maximum and spare respiration capacity compared to un-injected control (*Figure 8*). In addition, light exposure of A β -CRY2-mCh expressing embryos caused a significant reduction in ATP levels (*Figure 8a*).

Discussion

Aggregation of A β has been studied extensively, but our results represent the first study to demonstrate that induced oligomerization of intracellular A β can be used to separate different pathologies (induced by A β oligomerization vs expression alone). A second approach to making inducible aggregates using a chemically controlled fluorescent protein has been published, but not yet widely tested (*Miyazaki et al., 2016*). Other previous approaches lacked an inducible oligomerization tool and could only demonstrate A β oligomers' toxicity through exogenous injection of A β oligomers (*Mroczko et al., 2018*). We use a tool to investigate the pathological effects of intracellular A β oligomerization in nematodes and flies, human kidney cells, and in the vertebrate model organism zebrafish (*Figure 8—figure supplement 1, Video 4*). Despite the reversibility of CRY2 clustering in previous findings, we find that CRY2 initiated clustering of A β appeared to be irreversible likely due

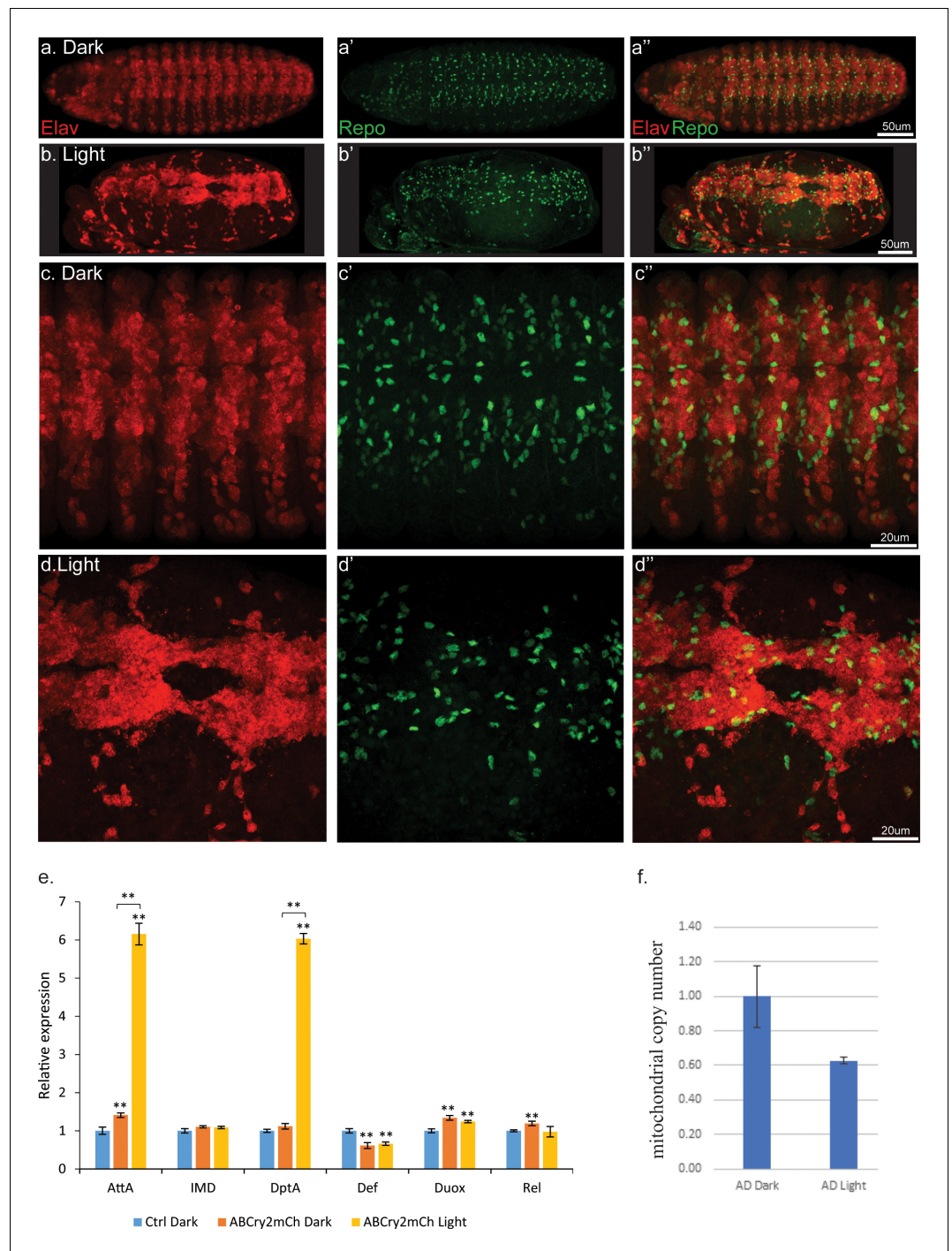
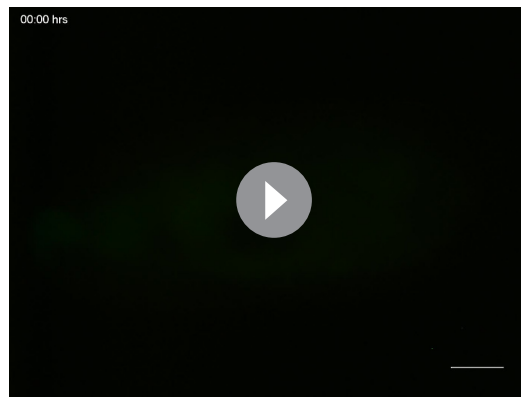


Figure 4. Light induced aggregation causes physical disruption of embryonic neural tissues. (a–a'') Elav-Gal4/UAS- $A\beta$ -CRY2-mCh embryos kept in the dark and imaged for neurons (Elav) and glial cells (Repo). (b–b'') Elav-Gal4/UAS- $A\beta$ -CRY2-mCh embryos exposed to light and imaged for neurons (Elav) and glial cells (Repo). (c–d'') Close ups. (E) Aggregation induced inflammatory response as measured by qPCR for inflammatory response genes. (f) The number of mitochondria in transgenic $A\beta$ *Drosophila* embryo was reduced by 40% in light. The online version of this article includes the following figure supplement(s) for figure 4:

Figure supplement 1. Light-induced $A\beta$ aggregation leads to developmental deficits in transgenic *Drosophila* embryo.



Video 3. Elav-Gal4/UAS-MyrTomato embryos exposed to light and imaged for neurons in red (tdTom) and glial cells Repo-QF2 >QUAS GFP. Blue laser power at higher setting to allow imaging of glial cells and control for laser damage.

<https://elifesciences.org/articles/52589#video3>

to the structure of the aggregates (*Antzutkin et al., 2012*). Consistent with existing literature showing that A β oligomers induce oxidative stress and inflammation (*Butterfield et al., 2013; Forloni and Balducci, 2018*), we show that light-induced oligomerization of A β , but not A β expression alone, is necessary for the metabolic defects, loss of mitochondria and inflammation in *C. elegans* and *Drosophila*. Light-induced oligomerization also leads to physical damage of the nervous system in *D. rerio*, resembling the loss of brain tissue in AD (**Figure 8—figure supplement 1**). The embryonic assay for physical damage phenocopies brain lesions only to some degree as the extent of the damage is enhanced by the forces applied to the developing neural tissue. The irreversibility of A β aggregates once initiated as seen here, also hints at intrinsic properties that may be unique or unusual to this peptide and warrants further investigation. It is also likely to prove a good model for testing anti-aggregation compounds.

We anticipate that our approach will serve as an attractive tool for carrying out drug screens and mechanistic studies for the treatment of AD. This optogenetic strategy will also undoubtedly complement other techniques due to the high level of spatiotemporal specificity. For example, it could be optimally positioned to gain insights into the unresolved mechanism of A β - whether oligomerization and subsequent accumulation or lack of effective clearance underpins AD pathologies. The separation of two phases of AD progression also suggests that single drug treatments will not suffice, and perhaps combinatorial approaches should be tried.

Materials and methods

Molecular cloning of optogenetic transgenes

DNA sequences corresponding to the human Amyloid β 1–42 amino acid sequence were synthesized (IDT) into a Gateway technology (Invitrogen) entry vector. The human A β 1–42 sequence was used for *Drosophila* and zebrafish due to close evolutionary conservation and a nematode-codon-optimized version of A β 1–42 was used for *C. elegans* (*Fong et al., 2016*). The CRY2-mCh fragment was cloned into pDONR vector with attB5 and attB2 sites, and MultiSite Gateway Pro 2.0 recombination (Invitrogen) was used to recombine donor plasmids and pDONR-CRY2-mCh into the respective destination vectors for three model organisms: a) pUASg.attB.3XHA for *Drosophila* to synthesize pUAS-A β -CRY2-mCh (*Bischof et al., 2007*) b) pDEST-hsp-16–2 p, a kind gift from Hidehito Kuroyanagi (Medical Research Institute, Tokyo Medical and Dental University) to synthesize hsp-16–2 p-A β -CRY2-mCh for *C. elegans* (*Okazaki et al., 2012*). c) pDEST-Tol2-PA2 (Invitrogen) and p5'E-Ubiquitin as described in *Kibat et al. (2016)* were used to make Ubiquitin driven pDEST-Tol2-PA2-Ubi-A β -CRY2-mCh and pDEST-Tol2-PA2 (Invitrogen) was used to make pDEST-Tol2-PA2-10xUAS-A β -CRY2-mCh for expression in *Danio rerio*. The CRY2 sequence were removed from this plasmid and the 10xUAS promoter were replaced with CMV promoter to produce pDEST-Tol2-PA2-CMV- A β -mCh by Gibson Assembly (NEB) for expression in *D. Rerio*.

d)pDEST40 (Invitrogen) was used to make CMV driven pDEST40-A β -CRY2-mCh for expression in HEK293 tissue culture cells.

Crosses and expression of UAS construct

For *Drosophila*, the transgenes were injected into attP2 (Strain#8622) P[CaryP]attP268A4 by BestGene Inc (California) (*Groth et al., 2004; Markstein et al., 2008*). Expression was driven by Elav-GAL4 the neuronal driver and two ubiquitous drivers armadillo-GAL4 and daughterless-GAL4

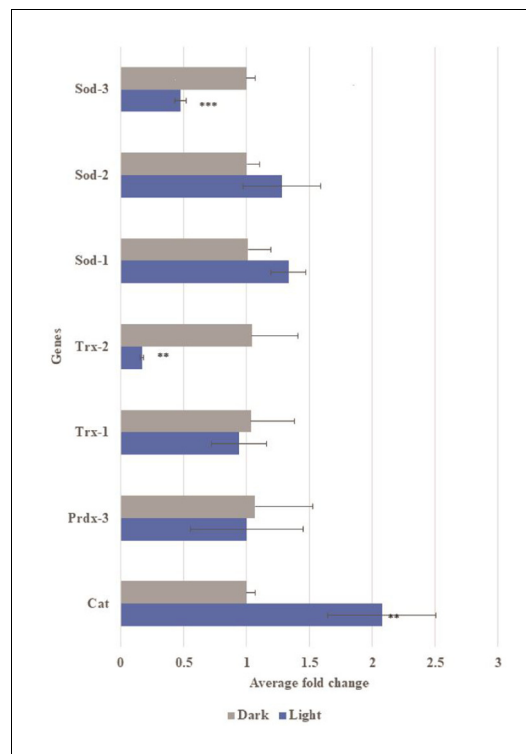


Figure 5. Gene expression of oxidative stress related genes in transgenic A β *C. elegans* with and without light-induction. Differential gene expression of catalase (Cat), peroxiredoxin-3 (Prdx3), thioredoxin-1 (Trx-1), thioredoxin-2 (Trx-2), superoxide dismutase-1 (SOD-1), superoxide dismutase-2 (SOD-2) and superoxide dismutase-3 (SOD-3) in transgenic A β *C. elegans* in light condition compared to control dark condition. Light-induced A β aggregation showed up-regulation in expression of Cat (** $p < 0.01$) and down-regulation in expression of Trx-2 (* $p < 0.01$) and Sod-3 (** $p < 0.001$).

(Brand and Perrimon, 1993). All additional stocks were obtained from the Bloomington *Drosophila* Stock Center (NIH P40OD018537) were used in this study.

Fly crosses performed were:

- Elav-Gal4 x w; UAS-A β -CRY2-mCh
- Arm-Gal4; Da-Gal4 x w; UAS-A β -CRY2-mCh
- Elav-Gal4; Repo-QF2, QUAS-GFP x UAS-A β -CRY2-mCh
- Elav-Gal4; Repo-QF2, QUAS-GFP x UAS-tdTomato
- esg-Gal4, UAS-GFP x w; UAS-A β -CRY2-mCh
- esg-Gal4, UAS-GFP x w; UAS-Arm-CRY2-mCh

For *C. elegans*, 50 ng/ μ l the construct hsp-16–2 p-A β -CRY2-mCh was co-injected with 25 ng/ μ l of pharyngeal-specific fluorescence marker *myo-2-gfp* into the distal gonads of wild type young adults. Transgenes were maintained as extrachromosomal arrays, hence careful selection of transgenic animals with pharyngeal GFP expression is required prior to all experiments. A *myo-2-gfp* strain *C. elegans* was also generated and used alongside as controls.

For *Danio rerio*, 50 ng/ μ l of the construct pDEST-Tol2-PA2-10xUAS-A β -CRY2-mCh and 60 ng/ μ l Tol2RNA transposase were injected into *TgBAC(gng8:GAL4)^{c416}* zebrafish embryos during the one-cell stage. pDEST-Tol2-PA2-Ubi-A β -CRY2-mCh and pDEST-Tol2-PA2-CMV-A β -mCh were injected into one-cell stage *mitfa^{-/-}* zebrafish embryos lacking melanin pigment separately.

Animal husbandry

Drosophila were maintained at standard humidity and temperature (25°C) with food containing 6 g Bacto agar, 114 g glucose, 56 g cornmeal, 25 g Brewer's yeast and 20 ml of 10% Nipagin in 1L final volume. Transgenic *Drosophila* and controls were distributed into either dark or light condition on Day 1. Transgenic flies fed with a lithium-supplemented diet were maintained in the same food as above with the addition of lithium chloride to a final concentration of 5 mM. *C. elegans* were maintained as previously described at 20°C (Stiernagle, 2006). Age-synchronized nematodes were generated by hypochlorite bleaching. 250 μ M of 5-fluoro-2'-deoxyuridine (FUDR) was added to prevent progeny production in all experiments except for fertility assays. For Fertility assay, normal Nematode Growth Media (NGM) agar plates were used. To induce expression of A β -CRY2-mCh, Day 4 young adult worms were heat shocked at 35°C for 90 min, and subsequently incubated at 20°C for a day (Day 5) for recovery. The heat-shocked transgenic Day 6 *C. elegans* were then separated into dark or light condition and was maintained at 20°C throughout the experimental period. Non-heat shock controls were used for lifespan, fertility and locomotion studies. Adult zebrafish were reared under standard zebrafish facility conditions with a 14 hr light/10 hr dark cycle. Zebrafish embryos injected with different expression vectors were screened for fluorescence and distributed into either dark or light condition 24 hr post fertilization. Embryos were dechorionated at 48 hr post fertilization and exposed to blue light (488 nM) for 1–2 hr at room temperature to induce oligomerization and subsequently used for mitochondria metabolic flux assay or ATP assay.

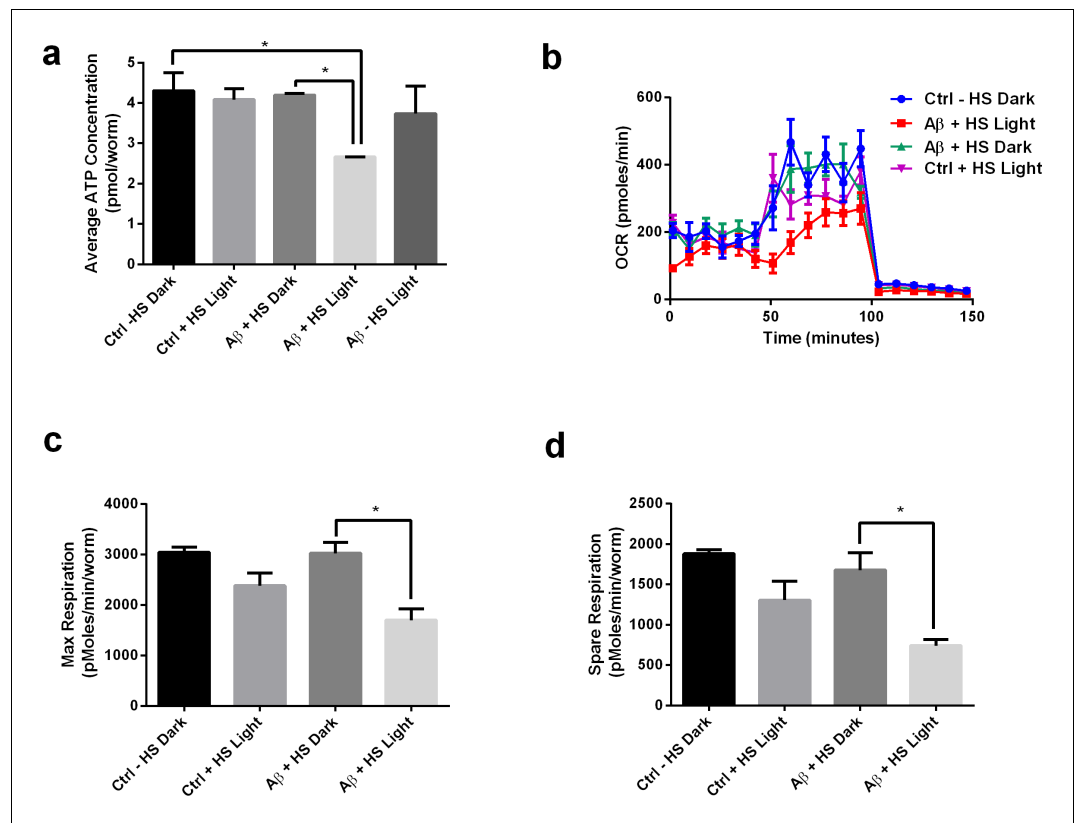


Figure 6. Light-induced A β oligomerization is required for the manifestation of metabolic defects in transgenic *C. elegans*. (a) ATP levels of control and transgenic A β nematodes ($n = 3$ repeats for each condition, with 100 nematodes per repeat; ANOVA post-test $p < 0.05$, *). (b) Oxygen consumption profile (OCR) of control and transgenic A β nematodes ($n = 6$ repeats for each condition, with 10 nematodes per repeat). (c) Maximal respiration derived from OCR ($n = 6$ repeats for each condition, with 10 nematodes per repeat; ANOVA post-test $p < 0.05$, *). (d) Spare respiration derived from OCR ($n = 6$ repeats for each condition, with 10 nematodes per repeat; ANOVA post-test $p < 0.05$, *).

FRAP assay

Adult fly midguts were dissected in 200 μ l of 1x PBS in a PYREX Spot Plates concave glass dish (FisherScientific). Subsequently, the guts were carefully transferred onto a small droplet of 1x PBS on a 35 mm glass bottom dish. Using fine forceps, the gut was repositioned to resemble its natural orientation. PBS was then removed from the area surrounding the gut, leaving a small amount of excess PBS to hold the gut in place and prevent desiccation. The 3 mm glass bottom dish was then mounted onto the Zeiss LSM800 (Carl Zeiss AG, Germany) for imaging. The super-resolution imaging function on the Zeiss LSM800 was used for the bleaching and fluorescence recovery. A small square within a cell was defined as the bleaching area and this same square was used for all bleaching experiments. Bleaching was performed at 4% laser power using the 488 nm laser for 1 s and the recovery was followed every 30 s for 20 minutes. The fluorescence intensity of the bleaching square (F_S), the entire cell (F_C) and the background (F_B) at each time point was computed by the ZEN 3.1 (Blue edition) software (Carl Zeiss, Germany). For determination of percentage fluorescence recovery, the background fluorescence was subtracted from the fluorescence of the bleaching square ($F_S - F_B$) and the fluorescence of the entire cell ($F_C - F_B$). The $(F_S - F_B) / (F_C - F_B)$ was computed at each time point and the $(F_S - F_B) / (F_C - F_B)$ before bleaching was set to 100%. This was done for all FRAP assays for both constructs and 3 separate experiments were conducted per construct.

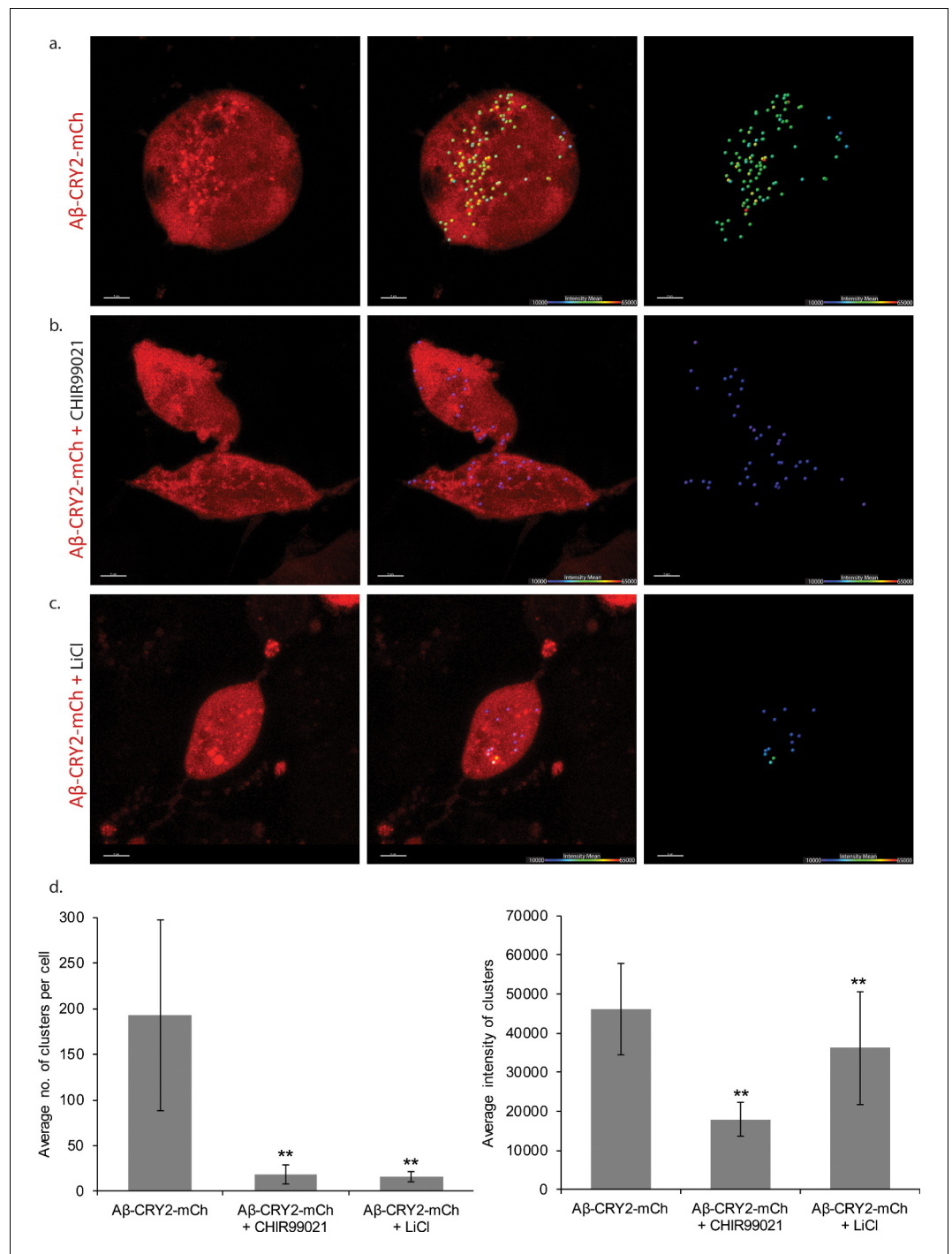
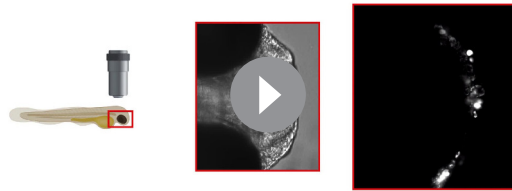


Figure 7. HEK cells expressing $A\beta$ -CRY2-mCh in light condition. (a) Untreated control HEK cells show light-induced clustering of $A\beta$ -CRY2-mCh and increased number of vacuoles under blue light illumination. (b) HEK cells treated with GSK3 inhibitor CHIR99021 (positive control) show little clustering of the light-induced $A\beta$ -CRY2-mCh. Fewer cellular vacuoles observed. (c) HEK cells treated with lithium chloride show homogenous expression of $A\beta$ -CRY2-mCh, whereby blue light illumination did not result in significant clustering of $A\beta$ -CRY2-mCh. (d) Quantification of cluster number per cell showed significantly reduced cluster formation in cells treated with CHIR99021 and lithium chloride as compared to control cells. (** $p < 0.01$) (e) Quantification of the mean intensity of the clusters showed significantly reduced intensity of the clusters when the cells were treated with GSK3 inhibitor CHIR99021 and lithium chloride as compared to control cells.



Video 4. Expression of A β -CRY2-mCh in zebrafish developing brains. Schematic of imaging set up and area of interest. Imaging of cell movement, A β -CRY2-mCh aggregation and cell death.

<https://elifesciences.org/articles/52589#video4>

1.5 cm internal diameter) and were tapped to the bottom. The number of *Drosophila* at the top (Ntop) of the column, and that at the bottom (Nbot) were counted after 20 s. Three trials with the same sample were performed within 30 s interval. Performance index was defined as (15+Ntop-Nbot)/30.

Heat-shocked *C. elegans* were assessed at Day 9, by placing worms onto individual NGM plates, pre-spotted with *Escherichia coli* OP50. *C. elegans* were placed on the side of the bacteria spot on the NGM plate using a platinum worm picker and were left undisturbed to move freely for 15 min. Distance travelled was determined by imaging and measuring of worm tracks on bacteria using a stereomicroscope.

Fertility assay

25 pairs of male and female *Drosophila* expressing MD-A β -Cry2-mCh were kept in a single tube under dark or light conditions. The number of eggs laid were scored after 5 hr 30 min for Days 5, 6, 7, 13, 14 and 20. Day 5 heat-shocked *C. elegans* were transferred onto individual NGM plates spotted with *E. coli*. Each worm was transferred to a fresh plate daily from Day 6 to Day 8, allowing 24 hr' egg laying period. The number of new young worms were counted on each plate as the progeny of a single individual.

Adenosine triphosphate (ATP) assay

ATP assay using firefly lantern extract (Sigma-Aldrich) was performed as described by *Tsujimoto et al. (1970)*. Each *C. elegans* sample containing 100 D2 adult worms was freeze-thawed in liquid nitrogen and sonicated in 10% Trichloroacetic acid (TCA) buffer while each zebrafish sample containing five 48hpf embryos was lysed in 10% TCA buffer. The extracted ATP from the different conditions and ATP standards were loaded onto a 96-well plate and injected with firefly lantern extract. Luminescence was measured using a Cytation 3 Imaging Reader (Biotek).



Video 5. Expression A β -mCh in zebrafish developing brains. Schematic of imaging set up and area of interest. No obvious cell movement or cell death despite A β -mCh expression.

<https://elifesciences.org/articles/52589#video5>

Lifespan assays

Drosophila and *C. elegans* were counted daily for the number of dead subjects and the number of censored subjects (excluded from the study). *Drosophila* that failed to respond to taps were scored as dead and those stuck to the food were censored. *C. elegans* that failed to respond to plate-tapping were scored as dead, those that burrowed to the side of the plate were censored.

Locomotion assay

Drosophila locomotion was assessed using an established geotaxis assay previous described in *Rival et al. (2009)*. In brief, 25 *Drosophila* were enclosed in a plastic column (25 cm tall, with a

Mitochondrial metabolic flux assay

Mitochondrial metabolic flux assay for *C. elegans* was performed as described by *Fong et al. (2017)* using XF96 Extracellular Flux Analyzer. 60 D2 adult worms from each condition 24 hr post light-treatment were transferred to a 96-well Seahorse plate containing M9 buffer. Final concentrations of the drugs used in the OCR experiment were 10 μ M FCCP and 50 mM sodium azide. For zebrafish embryos, mitochondrial metabolic flux assay was performed as described by *Stackley et al. (2011)* with some modifications. Oxygen consumption rate (OCR) measurements were performed using the XF96 Extracellular

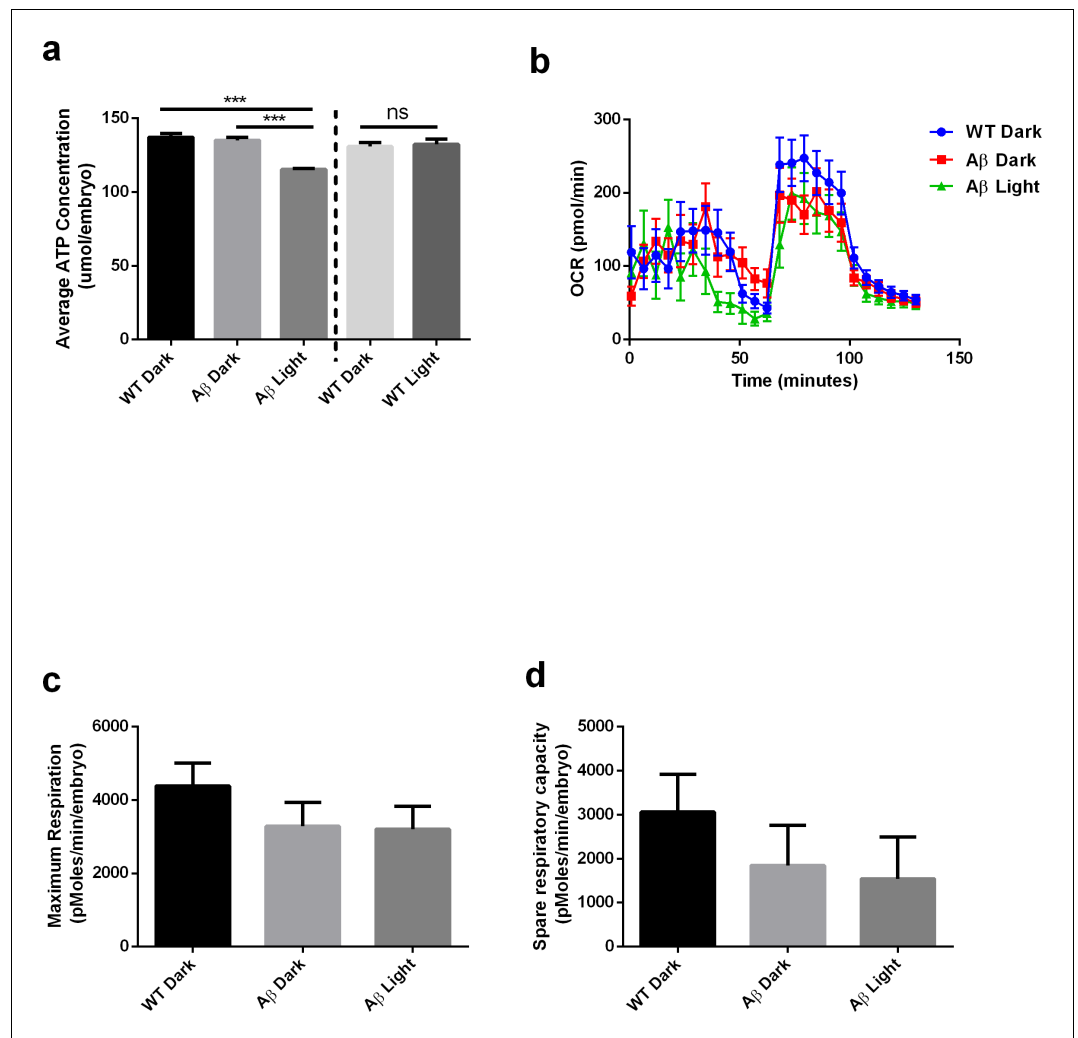


Figure 8. Light-induced A β oligomerization is required for the manifestation of metabolic defects in transgenic *D. rerio*. (a) ATP levels of control and transgenic A β *D. rerio* embryos ($n = 8$ repeats for each condition; ANOVA post-test $p < 0.001$, ***). Light treatment did not affect ATP levels in control embryos (performed in a separate experiment). (b) Oxygen consumption profile (OCR) of control and transgenic A β *D. rerio* embryos (24 embryos/condition) (c) Maximal respiration derived from OCR. (d) Spare respiration derived from OCR.

The online version of this article includes the following figure supplement(s) for figure 8:

Figure supplement 1. Transgenic A β model in *Danio Rerio* embryo expressing A β -CRY2-mCh (red).

Flux Analyzer. Each well contained one embryo (48hpf) in 175 μ L of E3 medium (fish system water). Final concentrations of the drugs used in the OCR experiment were 9.4 μ M oligomycin, 2.5 μ M FCCP and 20 mM sodium azide.

Light-sheet microscopy

Drosophila embryos were dechorionated using bleach, rinsed twice with water and dried, and loaded into a capillary filled with 1% low-melting agarose Type VII-A in water (Sigma) (Colosimo and Tolwinski, 2006). *C. elegans* and *D. rerio* were embedded directly in the agarose. Samples were imaged with a Lightsheet Z.1 microscope. Cry2 was activated by a dual-side illumination with 10% power 488 nm laser for 29.95 ms for every 2.5 min for 500 cycles. Controls were only exposed to 561 nm. Images were acquired with a water immersion objective at 10x/0.2 Illumination Optics and W Plan-Apochromat 20x/1.0 UV-VIS detection objective (Carl Zeiss, Germany). Image data were

processed using the maximum intensity projection function of ZEN 2014 SP software (Carl Zeiss, Germany), and were analyzed with ImageJ (NIH) and IMARIS 9.0 (Bitplane AG, UK).

Transfection and live cell confocal microscopy

Human Embryonic Kidney (HEK293T) cells were obtained from ATCC through the local distributor Bio-REV Pte Ltd after Short Tandem Repeat profiling, confirmed mycoplasma-free and maintained in Dulbecco's Modified Eagle's Medium with 10% Fetal Bovine Serum and 1% Penicillin and Streptomycin (Invitrogen). Cells were plated at 80% confluence on 35 mm TC treated glass bottom dish 24 hr prior to transfection with 2.5 mg of pDEST40-A β -CRY2-mCh using the Effectene Transfection Reagent (Qiagen). A transfection master mix containing the plasmid and transfection reagent was prepared for all treatment plates during each biological replicate to ensure the transfection efficiency was the same across all plates. Two hours after transfection, the control plate was topped up with 250 μ l of complete media without antibiotics. For cells treated with drugs, LiCl or CHIR99021 were also added at this point to achieve a final concentration of 2 mM LiCl or 3 mM CHIR99021 respectively. Cells transfected with only the pDEST40-A β -CRY2-mCh plasmid were used as negative control. Cells were imaged 24 hr after transfection using the Zeiss LSM800 confocal microscope with 63x oil immersion lens.

Immunofluorescence and confocal microscopy

Drosophila embryos 9 hr after deposition were incubated at 25°C in either light or dark conditions for 13 hr before being dechorionated using bleach. Embryos were then fixed with Heat-Methanol treatment (Müller and Wieschaus, 1996) or with heptane/4% formaldehyde in phosphate buffer (0.1M NaPO₄ pH 7.4) (Tolwinski and Wieschaus, 2001). Staining, detection and image processing as described in Colosimo and Tolwinski (2006).

Primary antibodies used were the glial cell marker anti-Repo (mouse mAb, 8D12) and the neuronal cell marker anti-Elav (rat mAb, 7EA810) from Developmental Studies Hybridoma Bank (DSHB) developed under the auspices of the NICHD and maintained by The University of Iowa, Department of Biological Sciences, Iowa City, IA 52242). Secondary antibodies used were Alexa Fluor 488 anti-rat and Alexa Fluor 647 anti-mouse (Invitrogen).

For detection of A β aggregates, thioflavin T (ThT) staining were performed as previously described Iijima et al. (2008). Formaldehyde-fixed embryos were incubated in 50% EtOH containing 0.1% ThT (Sigma) overnight. Embryos were destained in 50% EtOH for 10 min, followed by three washes in PBS. Embryos were then mounted on microscope slides using Aquapolymount (Polysciences, Inc).

Images were acquired on the Zeiss LSM 800 (Carl Zeiss, Germany) using the following settings: 1% laser power for 488 nm; 5% laser power for 561 nm; 2% laser power for 647 nm. Images were processed using the ZEN 2014 SP1 software (Carl Zeiss, Germany) and Imaris (Bitplane AG).

RNA extraction, cDNA synthesis and qPCR

Drosophila embryos 9 hr after deposition were incubated at 25°C in either light or dark conditions for 13 hr were used. Embryos were dechorionated and washed with 100% ethanol prior to RNA extraction using the ISOLATE II RNA Mini Kit's protocol (Bioline, UK). The extracted RNA was quantified using Nanodrop (Thermo Fisher Scientific). cDNA synthesis was done according to the SensiFAST cDNA Synthesis Kit's protocol (Bioline). Primers pairs used: AttA, IMD, DptA, Def, Duox, Rel, catalase, Prdx3, Trx1, Trx2, SOD-1, SOD-2, SOD-3 and reference gene Rpl32. Quantitative PCR was performed using SYBR Green. Expression data were normalized to the dark controls. For mitochondrial copy number, the above collection method was used except the following: the embryos were stored in tritonX-100 and the primers used were Mitochondria Cytochrome b (MtCyb) and reference gene RNase P.

Image data and statistical analysis

A β aggregates were quantified in *Drosophila* using ImageJ (NIH) and in *C. elegans* and HEK cells with IMARIS. For HEK cells, the number of clusters larger than 0.4 μ m in diameter were determined for at least 3 cells for the control and drug treated cells to calculate the average number of clusters per cell. The mean intensity per cluster across all these cells was also determined to calculate the

average intensity of the clusters for the control and drug treated cells. For statistical analysis of the expression of genes, student's t-test was used for except for cases where the data showed unequal standard deviation (F-test, $p < 0.05$), in which the Mann-Whitney nonparametric test was performed. Statistical analysis of lifespan studies and behavioral assays were performed using OASIS 2 (Han et al., 2016). The number of samples was determined empirically. All graphs were plotted using Graphpad PRISM 6 (Graphpad Software).

Key resources table

New model organisms generated for this paper are available to the community by contacting the authors. Stable lines and stocks will be made available through stock centers.

Drosophila line UAS-A β -Cry2-mCh inserted on Chromosome 3 site attP2:

- *D. rerio* UAS-A β -CRY2-mCh; TgBAC(*gng8:GAL4*)^{c416}
- *C. elegans* unintegrated line hsp-16-2 p-A β -CRY2-mCh.

Acknowledgements

We acknowledge Lavonna Mark and Rebecca Rubright for assistance with initial experiments using the zebrafish. We are thankful for the funding provided by Ministry of Education Singapore AcRF grant IG17-BS101 to JG, Yale-NUS College grant R-607-265-225-121 to ASM, AcRF grants IG17-LR006 and IG18-LR001 to NST.

Additional information

Funding

Funder	Grant reference number	Author
Ministry of Education - Singapore	IG17-LR001	Nicholas S Tolwinski
Ministry of Education - Singapore	IG17-BS101	Jan Gruber
Ministry of Education - Singapore	IG18-LR001	Nicholas S Tolwinski
Yale-NUS College	R-607-265-225-121	Ajay S Mathuru

The funders had no role in study design, data collection and interpretation, or the decision to submit the work for publication.

Author contributions

Chu Hsien Lim, Conceptualization, Investigation, Methodology; Prameet Kaur, Data curation, Investigation, Methodology; Emelyne Teo, Data curation, Validation, Investigation, Methodology; Vanessa Yuk Man Lam, Caroline Kibat, Investigation, Methodology; Fangchen Zhu, Investigation, Writing - original draft, Writing - review and editing; Jan Gruber, Resources, Supervision, Funding acquisition, Methodology; Ajay S Mathuru, Resources, Data curation, Supervision, Investigation, Methodology; Nicholas S Tolwinski, Conceptualization, Data curation, Formal analysis, Supervision, Funding acquisition, Investigation, Methodology

Author ORCIDs

Chu Hsien Lim [id https://orcid.org/0000-0001-6691-8277](https://orcid.org/0000-0001-6691-8277)

Emelyne Teo [id https://orcid.org/0000-0001-5050-4109](https://orcid.org/0000-0001-5050-4109)

Jan Gruber [id http://orcid.org/0000-0003-3329-3789](http://orcid.org/0000-0003-3329-3789)

Ajay S Mathuru [id http://orcid.org/0000-0003-4591-5274](http://orcid.org/0000-0003-4591-5274)

Nicholas S Tolwinski [id https://orcid.org/0000-0002-8507-2737](https://orcid.org/0000-0002-8507-2737)

Decision letter and Author response

Decision letter <https://doi.org/10.7554/eLife.52589.sa1>

Author response <https://doi.org/10.7554/eLife.52589.sa2>

Additional files

Supplementary files

- Transparent reporting form

Data availability

All data generated or analysed during this study are included in the manuscript and supporting files.

References

- Ahn NG, Nahreini TS, Tolwinski NS, Resing KA. 2001. Pharmacologic inhibitors of MKK1 and MKK2. *Methods in Enzymology* **332**:417–431. DOI: [https://doi.org/10.1016/s0076-6879\(01\)32219-x](https://doi.org/10.1016/s0076-6879(01)32219-x), PMID: 11305115
- Anderson RM, Hadjichrysanthou C, Evans S, Wong MM. 2017. Why do so many clinical trials of therapies for alzheimer's disease fail? *The Lancet* **390**:2327–2329. DOI: [https://doi.org/10.1016/S0140-6736\(17\)32399-1](https://doi.org/10.1016/S0140-6736(17)32399-1)
- Antzutkin ON, Iuga D, Filippov AV, Kelly RT, Becker-Baldus J, Brown SP, Dupree R. 2012. Hydrogen bonding in Alzheimer's amyloid- β fibrils probed by $^{15}\text{N}\{^{17}\text{O}\}$ REAPDOR solid-state NMR spectroscopy. *Angewandte Chemie* **51**:10289–10292. DOI: <https://doi.org/10.1002/anie.201203595>, PMID: 22976560
- Bischof J, Maeda RK, Hediger M, Karch F, Basler K. 2007. An optimized transgenesis system for *Drosophila* using germ-line-specific phiC31 integrases. *PNAS* **104**:3312–3317. DOI: <https://doi.org/10.1073/pnas.0611511104>, PMID: 17360644
- Brand AH, Perrimon N. 1993. Targeted gene expression as a means of altering cell fates and generating dominant phenotypes. *Development* **118**:401–415.
- Bugaj LJ, Choksi AT, Mesuda CK, Kane RS, Schaffer DV. 2013. Optogenetic protein clustering and signaling activation in mammalian cells. *Nature Methods* **10**:249–252. DOI: <https://doi.org/10.1038/nmeth.2360>, PMID: 23377377
- Bugaj LJ, Spelke DP, Mesuda CK, Varedi M, Kane RS, Schaffer DV. 2015. Regulation of endogenous transmembrane receptors through optogenetic Cry2 clustering. *Nature Communications* **6**:6898. DOI: <https://doi.org/10.1038/ncomms7898>, PMID: 25902152
- Bugaj LJ, Sabnis AJ, Mitchell A, Garbarino JE, Toettcher JE, Bivona TG, Lim WA. 2018. Cancer mutations and targeted drugs can disrupt dynamic signal encoding by the Ras-Erk pathway. *Science* **361**:eaao3048. DOI: <https://doi.org/10.1126/science.aao3048>, PMID: 30166458
- Butterfield DA, Swomley AM, Sultana R. 2013. Amyloid β -peptide (1-42)-induced oxidative stress in alzheimer disease: importance in disease pathogenesis and progression. *Antioxidants & Redox Signaling* **19**:823–835. DOI: <https://doi.org/10.1089/ars.2012.5027>, PMID: 23249141
- Castillo-Quan JI, Li L, Kinghorn KJ, Ivanov DK, Tain LS, Slack C, Kerr F, Nespital T, Thornton J, Hardy J, Bjedov I, Partridge L. 2016. Lithium promotes longevity through GSK3/NRF2-Dependent hormesis. *Cell Reports* **15**:638–650. DOI: <https://doi.org/10.1016/j.celrep.2016.03.041>, PMID: 27068460
- Colosimo PF, Tolwinski NS. 2006. Wnt, hedgehog and junctional Armadillo/beta-catenin establish planar polarity in the *Drosophila* embryo. *PLOS ONE* **1**:e9. DOI: <https://doi.org/10.1371/journal.pone.0000009>, PMID: 17183721
- Cummings J. 2018. Lessons learned from alzheimer disease: clinical trials with negative outcomes. *Clinical and Translational Science* **11**:147–152. DOI: <https://doi.org/10.1111/cts.12491>, PMID: 28767185
- Cummings J, Lee G, Ritter A, Zhong K. 2018. Alzheimer's disease drug development pipeline: 2018. *Alzheimer's & Dementia* **4**:195–214. DOI: <https://doi.org/10.1016/j.trci.2018.03.009>, PMID: 29955663
- De Ferrari GV, Chacón MA, Barria MI, Garrido JL, Godoy JA, Olivares G, Reyes AE, Alvarez A, Bronfman M, Inestrosa NC. 2003. Activation of wnt signaling rescues neurodegeneration and behavioral impairments induced by beta-amyloid fibrils. *Molecular Psychiatry* **8**:195–208. DOI: <https://doi.org/10.1038/sj.mp.4001208>, PMID: 12610652
- De-Paula VJ, Radanovic M, Diniz BS, Forlenza OV. 2012. Alzheimer's disease. *Sub-Cellular Biochemistry* **65**:329–352. DOI: https://doi.org/10.1007/978-94-007-5416-4_14, PMID: 23225010
- Duff K, Eckman C, Zehr C, Yu X, Prada CM, Perez-tur J, Hutton M, Buee L, Harigaya Y, Yager D, Morgan D, Gordon MN, Holcomb L, Refolo L, Zenk B, Hardy J, Younkin S. 1996. Increased amyloid-beta $_{42}$ (43) in brains of mice expressing mutant presenilin 1. *Nature* **383**:710–713. DOI: <https://doi.org/10.1038/383710a0>, PMID: 8878479
- Fenno L, Yizhar O, Deisseroth K. 2011. The development and application of optogenetics. *Annual Review of Neuroscience* **34**:389–412. DOI: <https://doi.org/10.1146/annurev-neuro-061010-113817>, PMID: 21692661
- Ferreira ST, Klein WL. 2011. The a β oligomer hypothesis for synapse failure and memory loss in Alzheimer's disease. *Neurobiology of Learning and Memory* **96**:529–543. DOI: <https://doi.org/10.1016/j.nlm.2011.08.003>, PMID: 21914486

- Fong S**, Teo E, Ng LF, Chen CB, Lakshmanan LN, Tsoi SY, Moore PK, Inoue T, Halliwell B, Gruber J. 2016. Energy crisis precedes global metabolic failure in a novel *Caenorhabditis elegans* alzheimer disease model. *Scientific Reports* **6**:33781. DOI: <https://doi.org/10.1038/srep33781>, PMID: 27653553
- Fong S**, Ng LF, Ng LT, Moore PK, Halliwell B, Gruber J. 2017. Identification of a previously undetected metabolic defect in the complex II *Caenorhabditis elegans* mev-1 mutant strain using respiratory control analysis. *Biogerontology* **18**:189–200. DOI: <https://doi.org/10.1007/s10522-016-9672-6>, PMID: 28039571
- Fonte V**, Kipp DR, Yerg J, Merin D, Forrestal M, Wagner E, Roberts CM, Link CD. 2008. Suppression of in vivo beta-amyloid peptide toxicity by overexpression of the HSP-16.2 small chaperone protein. *Journal of Biological Chemistry* **283**:784–791. DOI: <https://doi.org/10.1074/jbc.M703339200>, PMID: 17993648
- Forloni G**, Balducci C. 2018. Alzheimer's Disease, Oligomers, and Inflammation. *Journal of Alzheimer's Disease* **62**:1261–1276. DOI: <https://doi.org/10.3233/JAD-170819>, PMID: 29562537
- Groth AC**, Fish M, Nusse R, Calos MP. 2004. Construction of transgenic *Drosophila* by using the site-specific integrase from phage phiC31. *Genetics* **166**:1775–1782. DOI: <https://doi.org/10.1534/genetics.166.4.1775>, PMID: 15126397
- Guglielmi G**, Barry JD, Huber W, De Renzis S. 2015. An optogenetic method to modulate cell contractility during tissue morphogenesis. *Developmental Cell* **35**:646–660. DOI: <https://doi.org/10.1016/j.devcel.2015.10.020>, PMID: 26777292
- Han SK**, Lee D, Lee H, Kim D, Son HG, Yang JS, Lee SV, Kim S. 2016. OASIS 2: online application for survival analysis 2 with features for the analysis of maximal lifespan and healthspan in aging research. *Oncotarget* **7**: 56147–56152. DOI: <https://doi.org/10.18632/oncotarget.11269>, PMID: 27528229
- Hardy JA**, Higgins GA. 1992. Alzheimer's disease: the amyloid cascade hypothesis. *Science* **256**:184–185. DOI: <https://doi.org/10.1126/science.1566067>, PMID: 1566067
- Hawkes N**. 2016. Sixty seconds on . . . solanezumab. *BMJ* **355**:i6389. DOI: <https://doi.org/10.1136/bmj.i6389>
- Hong E**, Santhakumar K, Akitake CA, Ahn SJ, Thisse C, Thisse B, Wyart C, Mangin JM, Halpern ME. 2013. Cholinergic left-right asymmetry in the habenulo-interpeduncular pathway. *PNAS* **110**:21171–21176. DOI: <https://doi.org/10.1073/pnas.1319566110>, PMID: 24327734
- Huang A**, Amourda C, Zhang S, Tolwinski NS, Saunders TE. 2017. Decoding temporal interpretation of the morphogen bicoid in the early *Drosophila* embryo. *eLife* **6**:e26258. DOI: <https://doi.org/10.7554/eLife.26258>, PMID: 28691901
- Idevall-Hagren O**, Dickson EJ, Hille B, Toomre DK, De Camilli P. 2012. Optogenetic control of phosphoinositide metabolism. *PNAS* **109**:E2316–E2323. DOI: <https://doi.org/10.1073/pnas.1211305109>
- Iijima K**, Chiang HC, Hearn SA, Hakker I, Gatt A, Shenton C, Granger L, Leung A, Iijima-Ando K, Zhong Y. 2008. Abeta42 mutants with different aggregation profiles induce distinct pathologies in *Drosophila*. *PLOS ONE* **3**: e1703. DOI: <https://doi.org/10.1371/journal.pone.0001703>, PMID: 18301778
- Jin N**, Zhu H, Liang X, Huang W, Xie Q, Xiao P, Ni J, Liu Q. 2017. Sodium selenate activated wnt/ β -catenin signaling and repressed amyloid- β formation in a triple transgenic mouse model of Alzheimer's disease. *Experimental Neurology* **297**:36–49. DOI: <https://doi.org/10.1016/j.expneurol.2017.07.006>, PMID: 28711506
- Johnson HE**, Goyal Y, Pannucci NL, Schüpbach T, Shvartsman SY, Toettcher JE. 2017. The spatiotemporal limits of developmental erk signaling. *Developmental Cell* **40**:185–192. DOI: <https://doi.org/10.1016/j.devcel.2016.12.002>, PMID: 28118601
- Kasuya J**, Kaas G, Kitamoto T. 2009. Effects of lithium chloride on the gene expression profiles in *Drosophila* heads. *Neuroscience Research* **64**:413–420. DOI: <https://doi.org/10.1016/j.neures.2009.04.015>, PMID: 19410610
- Kaur P**, Saunders TE, Tolwinski NS. 2017. Coupling optogenetics and light-sheet microscopy, a method to study wnt signaling during embryogenesis. *Scientific Reports* **7**:16636. DOI: <https://doi.org/10.1038/s41598-017-16879-0>, PMID: 29192250
- Kennedy MJ**, Hughes RM, Peteya LA, Schwartz JW, Ehlers MD, Tucker CL. 2010. Rapid blue-light-mediated induction of protein interactions in living cells. *Nature Methods* **7**:973–975. DOI: <https://doi.org/10.1038/nmeth.1524>, PMID: 21037589
- Kerr F**, Sofola-Adesakin O, Ivanov DK, Gatliff J, Gomez Perez-Nievas B, Bertrand HC, Martinez P, Callard R, Snoeren I, Cochemé HM, Adcott J, Khericha M, Castillo-Quan JI, Wells G, Noble W, Thornton J, Partridge L. 2017. Direct Keap1-Nrf2 disruption as a potential therapeutic target for alzheimer's disease. *PLOS Genetics* **13**: e1006593. DOI: <https://doi.org/10.1371/journal.pgen.1006593>, PMID: 28253260
- Kerr F**, Bjedov I, Sofola-Adesakin O. 2018. Molecular mechanisms of lithium action: switching the light on multiple targets for dementia using animal models. *Frontiers in Molecular Neuroscience* **11**:297. DOI: <https://doi.org/10.3389/fnmol.2018.00297>, PMID: 30210290
- Khan A**, Jamwal S, Bijjem KR, Prakash A, Kumar P. 2015. Neuroprotective effect of hemoxygenase-1/glycogen synthase kinase-3 β modulators in 3-nitropropionic acid-induced neurotoxicity in rats. *Neuroscience* **287**:66–77. DOI: <https://doi.org/10.1016/j.neuroscience.2014.12.018>, PMID: 25536048
- Kibat C**, Krishnan S, Ramaswamy M, Baker BJ, Jesuthasan S. 2016. Imaging voltage in zebrafish as a route to characterizing a vertebrate functional connectome: promises and pitfalls of genetically encoded indicators. *Journal of Neurogenetics* **30**:80–88. DOI: <https://doi.org/10.1080/01677063.2016.1180384>, PMID: 27328843
- Klein PS**, Melton DA. 1996. A molecular mechanism for the effect of lithium on development. *PNAS* **93**:8455–8459. DOI: <https://doi.org/10.1073/pnas.93.16.8455>, PMID: 8710892
- Kumar A**, Singh A, Ekavali. 2015. A review on Alzheimer's disease pathophysiology and its management: an update. *Pharmacological Reports* **67**:195–203. DOI: <https://doi.org/10.1016/j.pharep.2014.09.004>, PMID: 25712639

- LaFerla FM**, Green KN, Oddo S. 2007. Intracellular amyloid-beta in Alzheimer's disease. *Nature Reviews Neuroscience* **8**:499–509. DOI: <https://doi.org/10.1038/nrn2168>, PMID: 17551515
- Licht RW**. 2012. Lithium: still a major option in the management of bipolar disorder. *CNS neuroscience & Therapeutics* **18**:219–226. DOI: <https://doi.org/10.1111/j.1755-5949.2011.00260.x>, PMID: 22070642
- Lim C**, Mathuru A. 2018. Modeling Alzheimer's and Other Age Related Human Diseases in Embryonic Systems. *Journal of Developmental Biology* **6**:1. DOI: <https://doi.org/10.3390/jdb6010001>
- Markstein M**, Pitsouli C, Villalta C, Celniker SE, Perrimon N. 2008. Exploiting position effects and the gypsy retrovirus insulator to engineer precisely expressed transgenes. *Nature Genetics* **40**:476–483. DOI: <https://doi.org/10.1038/ng.101>, PMID: 18311141
- Más P**, Devlin PF, Panda S, Kay SA. 2000. Functional interaction of phytochrome B and cryptochrome 2. *Nature* **408**:207–211. DOI: <https://doi.org/10.1038/35041583>, PMID: 11089975
- McColl G**, Killilea DW, Hubbard AE, Vantipalli MC, Melov S, Lithgow GJ. 2008. Pharmacogenetic analysis of lithium-induced delayed aging in *Caenorhabditis elegans*. *Journal of Biological Chemistry* **283**:350–357. DOI: <https://doi.org/10.1074/jbc.M705028200>, PMID: 17959600
- Miyazaki Y**, Mizumoto K, Dey G, Kudo T, Perrino J, Chen LC, Meyer T, Wandless TJ. 2016. A method to rapidly create protein aggregates in living cells. *Nature Communications* **7**:11689. DOI: <https://doi.org/10.1038/ncomms11689>, PMID: 27229621
- Möglich A**, Moffat K. 2010. Engineered photoreceptors as novel optogenetic tools. *Photochemical & Photobiological Sciences* **9**:1286–1300. DOI: <https://doi.org/10.1039/c0pp00167h>, PMID: 20835487
- Mroczo B**, Groblewska M, Litman-Zawadzka A, Kornhuber J, Lewczuk P. 2018. Amyloid β oligomers (A β Os) in Alzheimer's disease. *Journal of Neural Transmission* **125**:177–191. DOI: <https://doi.org/10.1007/s00702-017-1820-x>, PMID: 29196815
- Müller HA**, Wieschaus E. 1996. Armadillo, bazooka, and stardust are critical for early stages in formation of the zonula adherens and maintenance of the polarized blastoderm epithelium in *Drosophila*. *The Journal of Cell Biology* **134**:149–163. DOI: <https://doi.org/10.1083/jcb.134.1.149>, PMID: 8698811
- Okazaki A**, Sudo Y, Takagi S. 2012. Optical silencing of *C. elegans* cells with arch proton pump. *PLOS ONE* **7**:e35370. DOI: <https://doi.org/10.1371/journal.pone.0035370>, PMID: 22629299
- Park J**, Wetzel I, Marriott I, Dréau D, D'Avanzo C, Kim DY, Tanzi RE, Cho H. 2018. A 3D human triculture system modeling neurodegeneration and neuroinflammation in Alzheimer's disease. *Nature Neuroscience* **21**:941–951. DOI: <https://doi.org/10.1038/s41593-018-0175-4>, PMID: 29950669
- Parr C**, Mirzaei N, Christian M, Sastre M. 2015. Activation of the wnt/ β -catenin pathway represses the transcription of the β -amyloid precursor protein cleaving enzyme (BACE1) via binding of T-cell factor-4 to BACE1 promoter. *The FASEB Journal* **29**:623–635. DOI: <https://doi.org/10.1096/fj.14-253211>, PMID: 25384422
- Rival T**, Page RM, Chandraratna DS, Sendall TJ, Ryder E, Liu B, Lewis H, Rosahl T, Hider R, Camargo LM, Shearman MS, Crowther DC, Lomas DA. 2009. Fenton chemistry and oxidative stress mediate the toxicity of the beta-amyloid peptide in a *Drosophila* model of alzheimer's disease. *European Journal of Neuroscience* **29**:1335–1347. DOI: <https://doi.org/10.1111/j.1460-9568.2009.06701.x>, PMID: 19519625
- Stackley KD**, Beeson CC, Rahn JJ, Chan SS. 2011. Bioenergetic profiling of zebrafish embryonic development. *PLOS ONE* **6**:e25652. DOI: <https://doi.org/10.1371/journal.pone.0025652>, PMID: 21980518
- Stiernagle T**. 2006. *Maintenance of C. Elegans WormBook*. Oxford University Press. DOI: <https://doi.org/10.1895/wormbook.1.101.1>
- Tam ZY**, Gruber J, Ng LF, Halliwell B, Gunawan R. 2014. Effects of lithium on Age-related decline in mitochondrial turnover and function in *Caenorhabditis elegans*. *The Journals of Gerontology Series A: Biological Sciences and Medical Sciences* **69**:810–820. DOI: <https://doi.org/10.1093/gerona/glt210>
- Teo E**, Ravi S, Barardo D, Kim HS, Fong S, Cazenave-Gassiot A, Tan TY, Ching J, Kovalik JP, Wenk MR, Gunawan R, Moore PK, Halliwell B, Tolwinski N, Gruber J. 2019. Metabolic stress is a primary pathogenic event in transgenic *Caenorhabditis elegans* expressing pan-neuronal human amyloid beta. *eLife* **8**:e50069. DOI: <https://doi.org/10.7554/eLife.50069>, PMID: 31610847
- Teo E**, Fong S, Tolwinski N, Gruber J. 2020a. Drug synergy as a strategy for compression of morbidity in a *Caenorhabditis elegans* model of alzheimer's disease. *GeroScience* **1**:1. DOI: <https://doi.org/10.1007/s11357-020-00169-1>
- Teo E**, Lim SYJ, Fong S, Larbi A, Wright GD, Tolwinski N, Gruber J. 2020b. A high throughput drug screening paradigm using transgenic *Caenorhabditis elegans* model of Alzheimer's disease. *Translational Medicine of Aging* **4**:11–21. DOI: <https://doi.org/10.1016/j.tma.2019.12.002>
- Toledo EM**, Inestrosa NC. 2009. Activation of wnt signaling by lithium and rosiglitazone reduced spatial memory impairment and neurodegeneration in brains of an APP^{swe}/PSEN1 Δ E9 mouse model of Alzheimer's disease. *Molecular Psychiatry* **15**:272–285. DOI: <https://doi.org/10.1038/mp.2009.72>, PMID: 19621015
- Tolwinski NS**, Wieschaus E. 2001. Armadillo nuclear import is regulated by cytoplasmic anchor axin and nuclear anchor dTCF/Pan. *Development* **128**:2107–2117. PMID: 11493532
- Tsujimoto T**, Nakase Y, Sugano T. 1970. Firefly luminescence for ATP assay. *Wakayama Medical Reports* **14**:29–32. PMID: 5509591
- Westfall S**, Lomis N, Prakash S. 2018. Longevity extension in *Drosophila* through gut-brain communication. *Scientific Reports* **8**:8362. DOI: <https://doi.org/10.1038/s41598-018-25382-z>, PMID: 29849035
- Winblad B**. 1989. Bengt Winblad, geriatric researcher: the need for care increases with more and more people over the age of 80. *Lakartidningen* **86**:599–601. PMID: 2921903

- Wu Y**, Cao Z, Klein WL, Luo Y. 2010. Heat shock treatment reduces beta amyloid toxicity in vivo by diminishing oligomers. *Neurobiology of Aging* **31**:1055–1058. DOI: <https://doi.org/10.1016/j.neurobiolaging.2008.07.013>, PMID: 18762355
- Zarse K**, Terao T, Tian J, lwata N, Ishii N, Ristow M. 2011. Low-dose lithium uptake promotes longevity in humans and metazoans. *European Journal of Nutrition* **50**:387–389. DOI: <https://doi.org/10.1007/s00394-011-0171-x>, PMID: 21301855
- Zhang YW**, Thompson R, Zhang H, Xu H. 2011. APP processing in Alzheimer's disease. *Molecular Brain* **4**:3. DOI: <https://doi.org/10.1186/1756-6606-4-3>, PMID: 21214928